

3rd CIRP Conference on BioManufacturing

## Dimensional metrology of cell-matrix interactions in 3D microscale fibrous substrates

Filippos Tournomousis<sup>a</sup>, Robert C Chang<sup>a\*</sup>

<sup>a</sup>Stevens Institute of Technology, Castle Point on Hudson, Hoboken, NJ 07030

\* Corresponding author. Tel.:201-216-8301; fax: 201-216-8593. E-mail address: [rchang6@stevens.edu](mailto:rchang6@stevens.edu)

### Abstract

The significant potential of engineered tissue models is bounded by the current lack of robust scalable additive biomanufacturing processes that reliably capture the cell's structural microenvironments. To address this bottleneck, a melt electrospinning writing system is designed to fabricate 3D fibrous substrates within a tight cellular dimensional scale window. The biological relevance of the produced 3D experimental substrates over its 2D monolayer controls is demonstrated with respect to cell morphology. Cell confinement states are quantitatively characterized using an automated single-cell bioimage data analysis workflow. A multidimensional data set composed of size, shape and distribution related metrics of cellular and sub-cellular focal adhesions is extracted to build a classifier that can, with 91-93% classification accuracy, distinguish cell shape phenotypes in 3D confined versus 2D unconfined cell states.

© 2016 The Authors. Published by Elsevier B.V. This is an open access article under the CC BY-NC-ND license (<http://creativecommons.org/licenses/by-nc-nd/4.0/>).

Peer-review under responsibility of the scientific committee of the 3rd CIRP Conference on BioManufacturing 2017

**Keywords:** fiber; electrospinning; 3D; polymer; printing; biomanufacturing

### 1. Introduction

The fundamental requirement for reliably engineering biological systems is to recapitulate the cell's surrounding microenvironment, also known as the "cell niche" [1]. *In vivo*, human cells are suspended and confined within three-dimensional (3D) microenvironments defined by the porous microarchitecture of the native fibrous structure of the extracellular matrix (ECM) [2]. The role of the ECM extends beyond that of a static support structure for the cells, but also to provide cells with the appropriate mechanical and chemical signals that regulate and maintain their function [3]. Therefore, an enhanced understanding of the fundamental biological sciences, primarily the interplay between biological cells and ECM-related signals, demands a defined role for engineering design and manufacturing to meet the challenges presented by increasingly complex biological problems [4].

Additive Manufacturing (AM) in tissue engineering is the application of a suite of computer aided manufacturing process technologies towards the layered, patterned deposition of biological structures [3, 9]. The ability to precisely build

biopolymer melt substrates layerwise with subsequent biological cell cultivation has enabled their use as 3D biological systems. This intended use is based on the commonly held assertion that 3D substrates represent more physiologically-relevant models compared to their classical 2D counterparts. A reasonable question to ask is whether this assertion is a valid one. That is, does the 3D physical dimensionality of systems that are fabricated with classical 3D printing methods, induce natural responses to the seeded biological cells? It has been argued that 3D printed biomaterial substrates with geometrical feature sizes (fiber diameter and inter-fiber distance) larger than the cell's diameter (10 – 20  $\mu\text{m}$ ) cannot be considered reliable ECM-analogs since they promote cell growth on 2D with curvature [5], [6]. Thus, considering the limited resolution of classical 3D printing methods (>100  $\mu\text{m}$ ) and the fact that cell morphology is a potential indicator for cell function, the physiological relevance of classical 3D printed substrates indeed becomes questionable.

Several studies have reported the strong link between cell shape and cell function using adhesive micropatterning

techniques on 2D substrates. Furthermore, it has been shown that the dimensionality of the cell niche may indirectly control cell function through determination of cell shape on random nanofiber meshes [7], [8]. In addition, machine learning approaches have been employed to identify distinct cell shape metrics that can be used to elucidate morphological differences induced by random nanofibers meshes that promote distinct stem cell differentiation responses in both the absence and presence of bioactive growth factors [9].

In this paper, a high-resolution electrohydrodynamic-based 3D printing process known as melt electrospinning writing (MEW) is demonstrated to enable custom fabrication of high-fidelity 3D microscale fibrous biomaterial substrates that promote physiological 3D confined cell morphologies [15]. The biological relevance of the fabricated substrates is demonstrated by culturing human adherent cells and observing the resultant cell morphologies. The methodology advanced allows the extraction of cellular and subcellular morphometric features, including a wide variety of metrics for characterizing the shape-bearing focal adhesion (FA) proteins. Statistical analysis reveals that 3D microscale fibrous promote the most homogeneous cell shape phenotypic responses and that 3D confined states are characterized by less elliptical cell shapes, larger mean individual FA size and distinct FA distributions with respect to the unconfined states on the control substrates. An automated single-cell bioimage data analysis workflow is presented for multiscale morphological profiling. The extracted multidimensional single-cell feature datasets are used to build a classifier that can classify cell shape phenotypes to each substrate dimensionality.

## 2. High-Resolution 3D Printing Using MEW

### 2.1. Machine Design

A high-resolution 3D printing system configuration is established [10]–[12]. The process design is guided by detailed characterization of the properties governing the printability of the biomaterial. The overall system configuration is defined by three discrete process regimes (Figure 1). The polymer melt supply regime is composed of a glass Luer-lock syringe and a stainless-steel needle tip. The polymer melt is maintained in a uniform melt state using an industrial heat gun. In addition, a programmable syringe pump is mounted vertically and used to set the volumetric flow rate by adjusting the plunger speed within a syringe. The temperature is monitored both at the syringe barrel and the capillary tip with an infrared FLIR thermal camera (Figure 1b – upper part). Next, in the free-flow regime, a voltage potential is applied between the needle tip and the upper surface of a grounded electrically conductive collector (Figure 1b – lower part). Thirdly, in the collector regime, the grounded collector is mounted on an x-y programmable stage sequentially mounted on a lab jack. The tip to collector plate distance is monitored using a vertical digital meter. To compensate for ambient conditions that might affect the process, the overall system configuration is placed on an anti-vibrating optical table and contained within a plexiglass enclosure. Furthermore, the temperature and humidity values within the enclosure are monitored using multimeter equipped with a type K thermocouple.

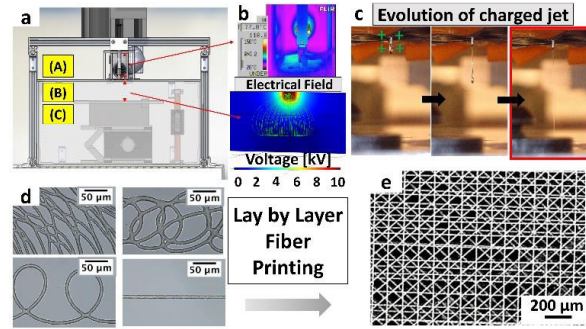


**Figure 1:** a) CAD model showing the 3 distinct process regimes: (A) Polymer supply regime, (B) Free-flow regime (C) Collector regime b) Upper part: The polymer supply regime is heated and monitored with a heat gun and thermal FLIR camera, respectively. Lower part: Numerical simulation of the electrical field lines and voltage potential map in the free-flow regime. c) Evolution of the charged jet in the free-flow regime with stretching of the extruded polymer melt jet. Optimization of the process parameters eliminates any instabilities arising from the electrical field and leads to printable straight charged jets. d) Various fiber topographies can be achieved by tuning the translational x-y stage speed. (Scale bar: 50  $\mu\text{m}$ ) e) 3D microscale fibrous structure by printing layer-by-layer aligned fibers with prescribed orientations. (Scale bar: 100  $\mu\text{m}$ )

### 2.2. Process optimization

Poly( $\epsilon$ -polycaprolactone), PCL is selected for the fabrication of the substrates on the basis of its FDA approval for *in vivo* applications and wide melt processing temperature window (60 – 90°C). The precise printing of fibrous mesh structures using the in-house built electrospinning writing process represents a process optimization challenge [24–26]. To address this challenge, the authors have previously defined a printability number,  $N_{PR}^*$ , which is defined based on a dimensional analysis framework that is correlated with the dimensionless parameters associated with the governing conservation equations [11]. In the present study, the same tuning procedure is established to determine an optimum printability number. At this setting, a combination of the applied voltage potential ( $V_p$ ) and the volumetric flow rate ( $Q$ ) setting promotes the balance of the downstream pulling with the upstream resistive forces to yield straight charged jets in the free-flow regime (Figure 1-c). This process parameterization, in tandem with the tuning of the translational stage speed ( $U_T$ ) at its critical value, yields a steady equilibrium printing state characterized by precise fiber placement of aligned fibers (Figure 1-d). As a result, layered fibrous meshes with well-defined pore architectures can be printed under optimum  $N_{PR}^*$  settings ( $V_p = 11$  kV,  $Q = 15$   $\mu\text{L/h}$ ,  $U_T = 60$  mm/s) for the prescribed melting conditions ( $T = 78$  °C) (Figure 1-e). PCL layered fibrous meshes are fabricated with an in-house melt electrospinning writing system (MEW). The enabling MEW process is performed by mounting the grounded aluminum collector on an automated x-y translational stage. PCL meshes with average fiber diameter equal to 10  $\mu\text{m}$  and 2 different pore microarchitectures (0-90° and 0°-45°-135°-90°) with average inter-fiber spacings of 150 and 75  $\mu\text{m}$ , respectively, are fabricated for this study.

Download English Version:

<https://daneshyari.com/en/article/5469634>

Download Persian Version:

<https://daneshyari.com/article/5469634>

[Daneshyari.com](https://daneshyari.com)